NOTES AND CORRESPONDENCE

Growth of Cloud Drops by Condensation: Effect of Surface Tension on the Dispersion of Drop Sizes

R. C. SRIVASTAVA

Laboratory for Atmospheric Probing, Department of the Geophysical Sciences, The University of Chicago, Chicago, Illinois

12 July 1990 and 20 February 1991

1. Introduction

The growth of cloud drops by condensation in an updraft has been treated in a number of papers starting with Howell (1949). Discussions of the subject may also be found in books (e.g., Mason 1971; Pruppacher and Klett 1978; Rogers and Yau 1989). For the case of a constant updraft, some of the salient results obtained by Howell and others by extensive numerical calculations may be summarized as follows. Initially, the supersaturation increases with time (or height above cloud base), reaches a maximum value (s_m at time t_m and height z_m, say), and thereafter decreases monotonically; at t_m, the nuclei divide into two groups—the ones with critical supersaturations less than or equal to s_m are activated and continue to grow, while those with greater critical supersaturations are not activated and slowly decrease in size. The drops growing on the former category of nuclei are usually referred to as cloud drops, while those formed on the latter category are called haze drops. Calculated cloud drop size distributions tend to be very narrow; in particular, the relative dispersion of the distribution, defined as the ratio of the standard deviation to the mean, decreases as condensation proceeds.

Two important parameters of the cloud drop size distribution are its width and the total concentration of the cloud drops. The width is important in considerations of the colloidal stability of the cloud, and the concentration is important in considerations of colloidal stability and optical properties of the cloud. In view of the highly nonlinear character of the equations governing the evolution of the size distribution of cloud drops by condensation, it is remarkable that approximate analytical results have been found for both quantities. The approximate solution for the concentration (Squires 1958b; Twomey 1959) relates it to the vertical air velocity and the nucleus size distribution. The approximate analytical result for the width of the distribution has been obtained by solution of an approximate form of the equation for cloud drop growth in which the effects of surface tension and dissolved nucleus on the equilibrium vapor pressure over drops containing activated nuclei are neglected (see, for example, Rogers and Yau 1989). According to this solution, the difference between the squared radii of any two given cloud drops remains constant after t_m irrespective of the vertical air velocity and the nucleus size distribution. This result implies that the variance of radius squared of the distribution also remains constant after t_m independent of the vertical air velocity and the nucleus size distribution.

In this study, we obtain another approximate analytical solution for the width of the cloud drop size distribution. The new result will be an improvement on the above result in that the effect of surface tension on the equilibrium vapor pressure over a drop will not be neglected even after t_m. It will be shown that because of the surface tension effect both the difference of the squared radii of any two cloud drops and the variance of the squared radius of the distribution do not remain constant but rather increase with the progress of condensation. The increase will be related to the vertical air velocity, the drop concentration, and the nucleus distribution. The approximate analytical result will be verified by numerical solution of the equations for the growth of cloud drops by condensation in which both surface tension and solute effects will be included. Both the numerical and analytical results will show that the magnitude of the increase of the variance of the squared radius of the distribution is not always small; indeed, it may have significant consequences for considerations of colloidal stability of warm clouds, especially at small values of the vertical air velocity. This also means that numerical cloud models in which the microphysics of condensation are approximated by neglecting the surface tension and solute effects (for example, Hall 1980; Song and Marwitz 1989) may be seriously in error. Based on the approximate solution for the width obtained here, an improved method for including the microphysics of condensation in numerical cloud models

Corresponding author address: Dr. R. C. Srivastava, Professor of Meteorology, The University of Chicago, Dept. of Geophysical Sciences, 5734 S. Ellis Avenue, Chicago, IL 60637.

will be outlined. Another new result, which will emerge from the numerical calculations, is that the previously accepted result that the concentration of cloud drops remains constant after t_m needs to be modified; this is because some of the nuclei activated before and up to time t_m may be subsequently deactivated, especially in weak updrafts.

The plan of presentation is as follows. In the next section, we shall present the basic equations for the growth of cloud drops by condensation and a short review of the earlier approximate analytical result on the width of the cloud drop size distribution; this will be followed by a derivation of the improved result for the width of the distribution. Section 3 will compare the results of the analytical solution with those of numerical calculations; examples of the magnitude of the effect of surface tension on the width of the distribution and its dependence on the vertical air velocity will also be given. In section 4, we will use the present results to discuss the colloidal stability of warm clouds and outline a method of using the results to improve the simulation of the microphysics of the condensation process in numerical cloud models. A summary of the results will be given in section 5.

2. Theory

a. Review

We shall consider growth of cloud drops by condensation in a closed parcel; this means, for example, that mixing of environmental air will not be considered. We shall use the following simplified form of the equation for the growth of cloud drops by condensation:

$$r\frac{dr}{dt} = c(s - s_{eq}). \tag{1}$$

For the ambient supersaturation, s, we shall use the macroscopic value (Srivastava 1989) given by

$$\frac{ds}{dt} = a_1 w - a_2 \frac{dl}{dt}. \tag{2}$$

In the above, r is the drop radius, t is time, s_{eq} is the equilibrium supersaturation over the drop, w is the vertical air velocity and l is the cloud water mixing ratio. Further,

$$\frac{1}{c} = \frac{\rho_w}{D\rho_a}\left[\frac{1}{\mu_s} + \frac{\lambda_1 L}{c_p}\frac{D}{\kappa}\right] \tag{3}$$

$$a_1 = \lambda_1\gamma_d - \lambda_2, \quad a_2 = \frac{1}{\mu_s} + \frac{\lambda_1 L}{c_p} \tag{4}$$

where

$$\lambda_1 = \frac{L}{R_v T^2}, \quad \lambda_2 = \frac{g}{R_d T}, \quad \gamma_d = \frac{g}{c_p}. \tag{5}$$

The equilibrium supersaturation is given by

$$s_{eq} = \frac{P}{r} - \frac{QM}{r^3} = \frac{P}{r}\left[1 - \left(\frac{r_c^2}{3r^2}\right)\right], \quad P = \frac{2\sigma}{\rho_w R_v T}. \tag{6}$$

The other symbols occurring above are ρ_w, the density of water; μ_s, the saturation vapor mixing ratio; L, the latent heat of vaporization of water; c_p, the specific heat of air at constant pressure; D, the diffusivity of water vapor in air; κ, the thermal diffusivity of air; ρ_a, the density of air; R_v and R_d, the specific gas constants for water vapor and air, respectively; and g, the gravitational acceleration. Equation (6) expresses the effects of surface tension and dissolved nucleus on s_{eq}. In it, r_c is the critical radius of the nucleus, σ is the surface tension of water, M is the mass of the nucleus, and Q is a parameter that depends upon the chemical composition of the nucleus. An explicit expression for Q will not be needed.

The approximate analytical solution for the width of the distribution, mentioned in the Introduction, may be derived as follows. In this derivation s_{eq} is neglected compared to s on the right-hand side of Eq. (1) for nuclei which are activated and continue to grow beyond their critical radii. If we consider two activated nuclei, distinguishing their radii by subscripts 1 and 2, then under this approximation, we have from (1):

$$r_2\frac{dr_2}{dt} - r_1\frac{dr_1}{dt} = 0, \tag{7}$$

which yields

$$\Delta \equiv r_2^2 - r_1^2 = \text{const.} \tag{8}$$

Thus, after time t_m, the difference of squared radii of any two activated nuclei does not change with the time. This implies that with the progress of condensation the concentration density of cloud drops plotted as a function of the squared radius simply translates to the right along the squared radius axis (see the thin full curves in Fig. 1 labeled t_0 and t; the thick curve labeled t will be discussed later). Therefore, we also have that

$$\text{var}(r^2) = \text{const} \tag{9}$$

where var stands for variance. This result can be used to deduce the size distribution of the cloud drops as a function of the time, if the distribution is given at one time (henceforth, most times considered will be after t_m). These points are discussed by East (1957) and Rogers and Yau (1989, pp. 104 and 111); a discussion of the analytical derivation of the size distribution under (8), and more general conditions, is given by Kovetz (1969).

b. Derivation of a new solution for the width of the distribution

We now obtain an improvement on Eqs. (7) through (9) by retaining the effects of surface tension even after

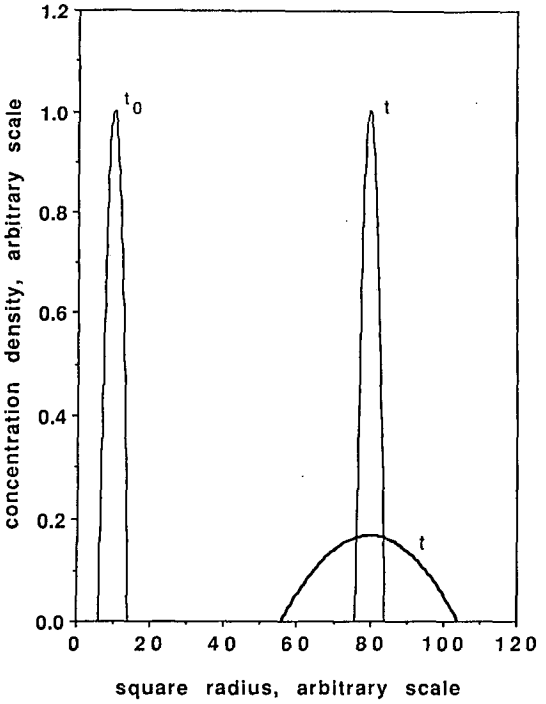

FIG. 1. Schematic figure showing the effect of surface tension on the width of the cloud drop size distribution. The curve labeled t_0 shows an initial distribution after the point of maximum supersaturation. The thin curve labeled t shows the distribution at a later time under the assumption that the effects of surface tension and solute on the equilibrium vapor pressure over drops may be neglected after t_0; in this case, the width of the distribution remains constant. If the surface tension is included, the distribution becomes wider as shown by the thick curve labeled t. In this illustration, it is assumed that between t_0 and t, the difference between the squared radii of any two given drops has increased by a factor of 6. The total concentration of cloud drops is not changed by condensation; therefore, the area under all the curves should be equal; as a result the thick curve is lower than the other two curves. All scales are arbitrary.

t_m. First, we shall show qualitatively that the difference between the squared radii of any two given activated nuclei may be expected to increase with time, rather than remaining constant, when the term s_{eq} in Eq. (1) is not neglected. For this discussion refer to Fig. 2; it shows schematically two curves, labeled s_{eq} and also A and B, of the equilibrium supersaturation over two nuclei (designated A and B) as a function of their radii; the curve labeled s shows the ambient supersaturation as a function of the time for $t > t_m$. Notice that the curve marked s has a different abscissa scale. Further, nucleus A has been assumed to have a higher critical supersaturation. Suppose at time t (point C), nuclei A and B have radii r_1 and r_2, respectively, as shown in the figure. We must have $r_2 > r_1$ because nucleus B (subscript 2) has a smaller critical supersaturation; therefore $(s - s_{eq})$ is larger for nucleus B; hence, the right-hand side of Eq. (7) will be greater than zero when s_{eq} is not neglected. This means that, rather than remaining constant, $r_2^2 - r_1^2$ and $\mathrm{var}(r^2)$ will both increase with the time. It is also easy to see that the curvature effect must be primarily responsible for this. This is because the curvature component of s_{eq} is much greater than the solute component for drop radii exceeding the critical radius. Indeed, we see from Eq. (6) that the ratio of the curvature to the solute term is $r_c^2/(3r^2)$, which is equal to ⅓ when the drop radius equals the critical radius and decreases rapidly with the radius becoming less than 0.1 for drop radii exceeding twice the critical radius.

We shall now quantify the above argument. For the reasons already given, we shall retain the effect of the surface tension but neglect that of the solute on the equilibrium vapor pressure over a drop after time t_m. Taking the difference of Eq. (1) for the two nuclei, we have instead of (7):

$$r_2 \frac{dr_2}{dt} - r_1 \frac{dr_1}{dt} = cP\left(\frac{1}{r_1} - \frac{1}{r_2}\right) \tag{10}$$

or

$$\frac{d \ln \Delta}{dt} = \frac{2cP}{r_1 r_2 (r_1 + r_2)}. \tag{11}$$

In the above, it is assumed, as in Fig. 2, that the drop with subscript 1 has the nucleus with the greater critical supersaturation. On the right-hand side, we now ap-

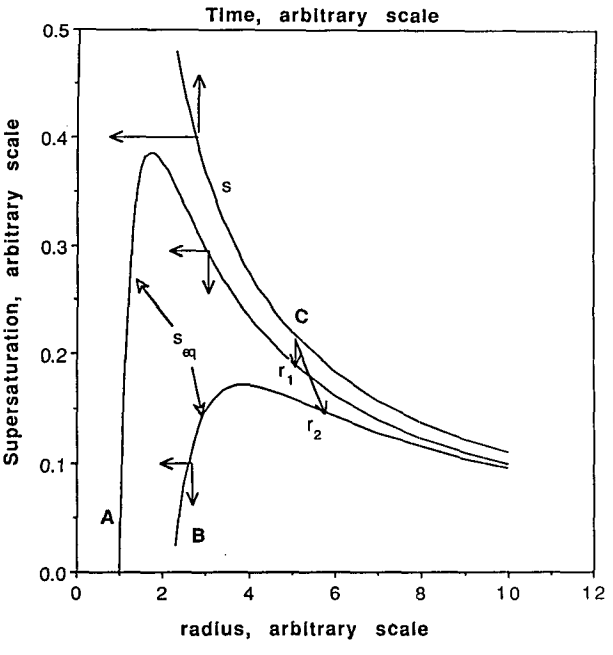

FIG. 2. Schematic figure explaining the role of the effect of surface tension on the equilibrium vapor pressure over drops in increasing the width of the distribution. Curves labeled s_{eq} show the equilibrium supersaturation over drops growing on two nuclei (labeled A and B) as a function of the drop radius (bottom axis). The curve labeled s shows the ambient supersaturation as a function of the time (top axis). All scales are arbitrary. For explanation, see text.

proximate r_1 and r_2 by the average volume radius r_* of the distribution. This is a good approximation because the cloud drop size distribution is very narrow. The radius r_* is related to the total drop concentration N and the cloud water mixing ratio l by

$$l = \frac{4\pi\rho_w}{3} N r_*^3. \tag{12}$$

From Eqs. (11) and (12), we have

$$\frac{d\ln\Delta}{dt} = \frac{4\pi\rho_w}{3}\frac{NcP}{l}. \tag{13}$$

As time increases, the cloud water content is well approximated by its adiabatic value, which we shall denote by l_a. Using Eq. (2), we have:

$$l \approx l_a \approx \frac{a_1}{a_2} z = \frac{a_1 w}{a_2} t. \tag{14}$$

In the above, we have taken the origins of z and t at the cloud base and have assumed a_1/a_2 to be approximately constant; this should be a good approximation if the depth of the cloud considered is not too great. In writing the last member of Eq. (14), we have also assumed that the vertical air velocity is constant. Integrating (13), assuming cP is also constant, we have

$$\frac{\Delta(t)}{\Delta(t_0)} = \left(\frac{l_a(t)}{l_a(t_0)}\right)^\delta = \left(\frac{t}{t_0}\right)^\delta = \left(\frac{z}{z_0}\right)^\delta \tag{15}$$

where

$$\delta \equiv cP\frac{4\pi\rho_w}{3}\frac{a_2}{a_1}\frac{N}{w}. \tag{16}$$

It also follows from the above that

$$\frac{\mathrm{var}(r^2)}{\mathrm{var}(r^2)_0} = \left(\frac{l_a}{l_{a0}}\right)^{2\delta} = \left(\frac{t}{t_0}\right)^{2\delta} = \left(\frac{z}{z_0}\right)^{2\delta}. \tag{17}$$

In the above, the quantities with the subscript 0 are for an initial time $t_0 > t_m$.

First, we note that if the effect of surface tension is neglected by putting $P = 0$, then we recover the Eqs. (8) and (9) from Eqs. (15) and (17), respectively. When P is not equal to zero, the difference of squared radii and the variance increase as a power of the height or time; the parameter δ gives a measure of the rate of increase, a greater δ implying a greater rate of increase. From Eq. (16), we see that the exponent δ increases with increasing N and decreasing w. Therefore, the effect of the surface tension in increasing the variance of square radius increases with increasing drop concentration and decreasing vertical air velocity. This is physically plausible because other things being the same: 1) the average radius decreases with increasing N which makes the surface tension effect (P/r) greater and 2) the ambient supersaturation decreases with decreasing w, which makes s_{eq} more comparable with s. However, the concentration and vertical air velocity are not independent, because the former is determined by the latter and the nucleus distribution; therefore, δ can be expressed in terms of the vertical air velocity and the nucleus distribution. For example, consider the power-law supersaturation spectrum of nuclei,

$$\eta = \alpha s^\beta = \alpha_{\%} s_{\%}^\beta, \quad \alpha_{\%} = \alpha 100^\beta \tag{18}$$

where η is the concentration of nuclei active at supersaturation s, α and β are constants, and $\alpha_{\%}$ is the value of α when s is expressed as a percentage, $s_{\%}$. It may be mentioned that the spectrum (18) is supported by observations (for example, Pruppacher and Klett 1978, p. 226). As shown by Twomey (1959), N is given approximately by

$$N = k\alpha^{2/(\beta+2)} w^{3\beta/(2\beta+4)} \tag{19}$$

where

$$k = \left[2\pi\rho_w \beta B\left(\frac{3}{2}, \frac{\beta}{2}\right)\right]^{-\beta/(\beta+2)} \times \left[\left(\frac{a_1}{c}\right)^{3/2}\frac{1}{a_2}\right]^{\beta/(\beta+2)}. \tag{20}$$

Here B stands for the beta function. From (16) and (19), we have

$$\delta = cP\frac{4\pi\rho_w}{3}\frac{a_2}{a_1} k \frac{\alpha^{2/(\beta+2)}}{w^{(4-\beta)/(2\beta+4)}}. \tag{21}$$

This gives the exponent δ in terms of the vertical air velocity, and the parameters α and β of the nucleus distribution and various coefficients occurring in the condensational growth equations.

In the above, the vertical air velocity was assumed to be constant. The case of a variable updraft can be treated similarly, although a solution in closed form will not be possible for arbitrary variations of the vertical air velocity. In section 4b, we shall give the solution for the case of a piecewise linear variation of the vertical air velocity.

3. Comparison of results of theory and numerical calculations

To demonstrate the validity of the new approximate analytical solution for the width of the distribution, we have integrated Eqs. (1) through (6) (supplemented by equations for the temperature and pressure) numerically for a large number of cases. For all cases, the continuous nucleus distribution (18) was approximated by a discrete distribution with 120 molar mass size categories spaced uniformly from 10^{-19} to 3×10^{-15} g on a logarithmic scale (the corresponding critical radii range from 3.36×10^{-6} μ to 5.83×10^{-4} μ). In all cases the cloud base temperature and pressure were taken as 283 K and 850 mb. The initial radii of

the drops at cloud base were prescribed rather arbitrarily as follows: first, the nuclei were brought to equilibrium with an atmosphere of relative humidity 70%, then they were allowed to grow in an atmosphere of relative humidity 100% for 5 minutes. Most of the nuclei then attained their equilibrium sizes appropriate to a relative humidity of 100%; only the largest nuclei exhibited a small lag and were slightly smaller than their equilibrium sizes. The results presented here should be quite independent of this initialization. (However, this may not be the case if a distribution with appreciable concentrations of nuclei with much larger critical radii is considered.) The equations were integrated forward in time until the parcel reached a height of 3 km. It is well known that in integrating Eq. (1), it is necessary to take very small time steps for the unactivated nuclei, while much larger time steps may be used for the activated nuclei (see, for example, Johnson 1980). To achieve computational efficiency, much of the previous work assumed the unactivated nuclei to be in equilibrium with the prevailing ambient supersaturation so that it was not necessary to solve (1) for those nuclei. We have not made this assumption. To maintain computational efficiency, we have used a small time step only for the unactivated nuclei. This small time step was taken to be a submultiple of the much larger time step used for the activated nuclei. That is, the calculations for the unactivated nuclei were done more frequently than for the activated nuclei. In this way the lag from equilibrium of the unactivated nuclei was maintained in the calculations without increasing the computational load too much.

Calculations for the different cases involved different values of the vertical air velocity and the parameters α and β. Results for two selected cases are presented in Figs. 3 and 4. In each of these cases the nucleus distribution parameters are $\alpha = 3.5 \times 10^9$ kg^{-1} and $\beta = 0.8$. Part (a) of each figure shows the radii for selected nuclei categories and the ambient supersaturation as a function of time. The time axis is the actual time plus 1 sec so that conditions at cloud base ($t = 0$) could also be displayed on the logarithmic scale. Because 1 sec has been added to the time scale, the height scale at the top is not proportional to the time scale; this is especially obvious near the point representing the cloud base ($z = 0$). Part (b) of each figure shows the radius-squared difference (Δ) as a function of the time. The radius-squared differences plotted are $r_k^2 - r_j^2$, where the subscript j refers to the smallest activated nucleus category (that is not subsequently deactivated) and k refers to the selected categories of activated nuclei plotted in part (a) of the figures.

Figure 3 is for a vertical air velocity of 6 m s^{-1}. Size category 35 is the smallest nucleus category activated. In Fig. 3b we see that the Δ curves are almost parallel *sloping* straight lines, which supports Eq. (15). If surface tension and solute effects had been neglected, we would have obtained straight lines parallel to the hor-

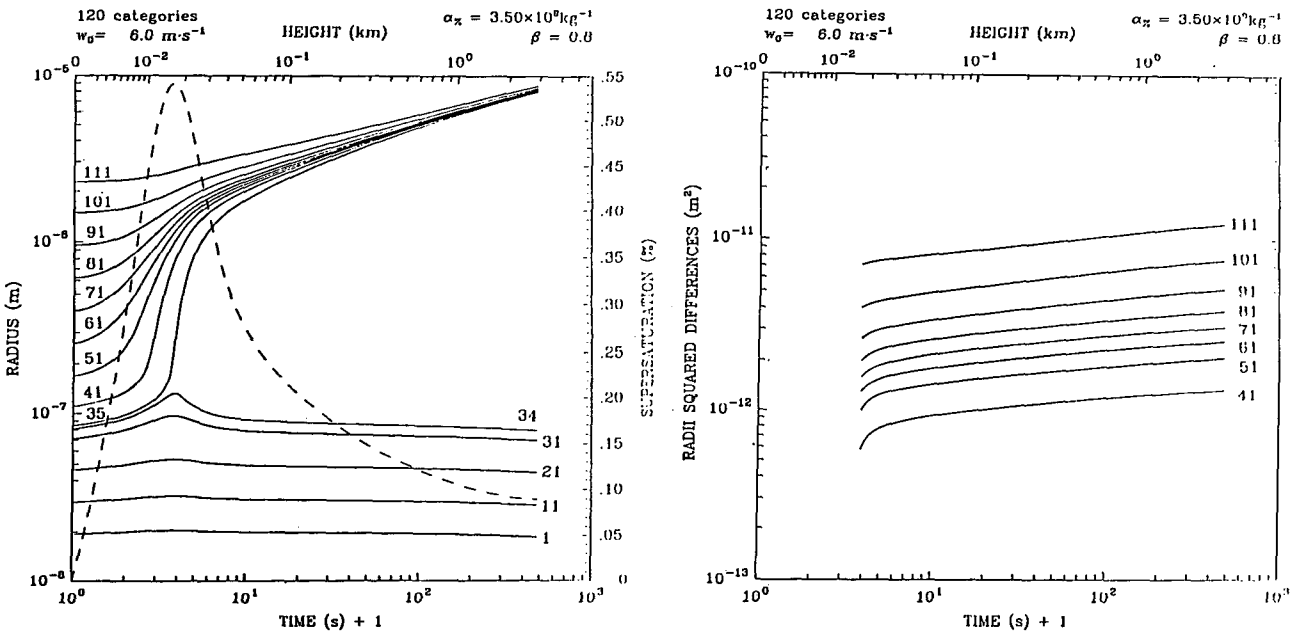

FIG. 3. (a) Plot of drop radii (solid lines) as function of the time for drops growing on selected categories of nuclei as shown on the curves. The dashed curve shows the supersaturation as a function of the time. Note that 1 second has been added to all the times to enable plotting of points at the cloud base ($t = 0$) on the logarithmic scale. The top axis shows height above cloud base. (b) Differences between squared radii of activated drops of nucleus categories marked on the curves and the squared radius of the drop growing on the smallest category (35) of activated nucleus as a function of the time. The vertical air velocity and the coefficient and exponent of the power-law nucleus supersaturation spectrum are shown at the top. The vertical air velocity is 6 m s^{-1}.

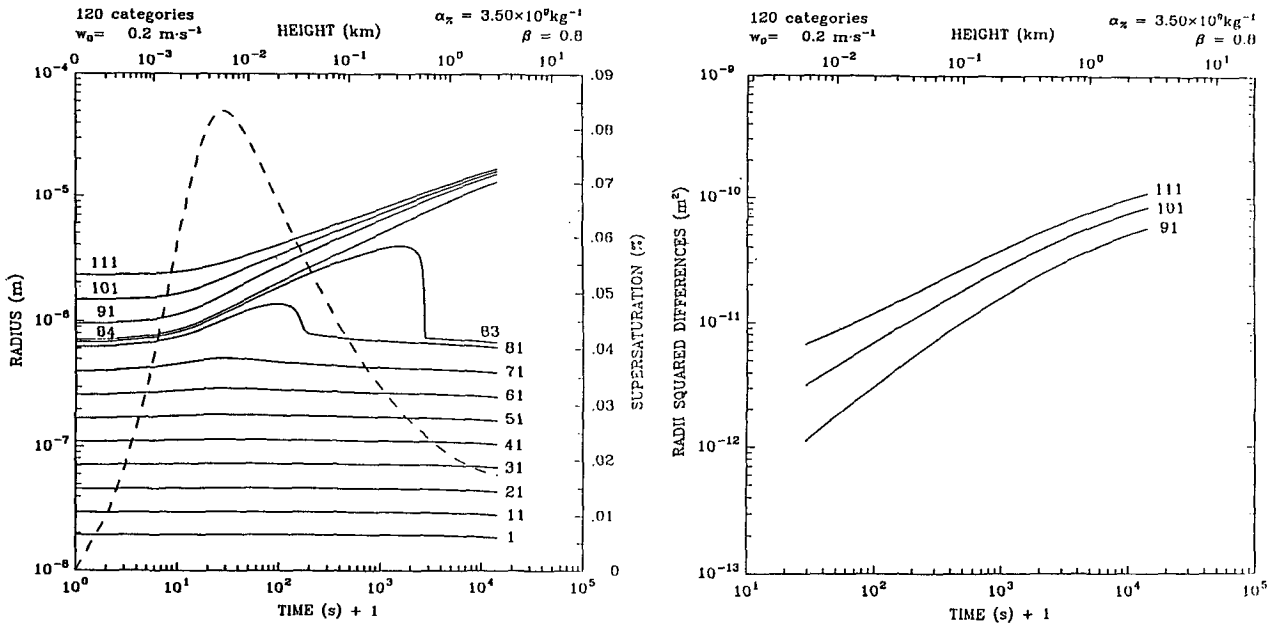

FIG. 4. Similar to Fig. 3 but for a vertical air velocity of 0.2 m s^{-1}.

izontal axis. Small deviations from the predicted behavior occur near t_m and are more pronounced for the smaller nuclei. These deviations are due to the neglect of the solute effect and the approximation that the actual water content and its height derivative are equal to their adiabatic values. These assumptions are generally most strongly violated near t_m.

Figure 4 shows results for a weak updraft of 0.2 m s^{-1}. In this case, the smallest nucleus category activated is 84. Part (b) of the figure shows that the Δ curves are again approximately parallel straight lines supporting Eq. (15). However, in this case the agreement with the theory is not as good as in the previous case; this is because with the lower vertical air velocity the ambient supersaturation and the equilibrium supersaturations over the drops are much closer to each other. It may be noted that sedimentation effects, which have not been considered may be important in this case because of the weak vertical air velocity.

A more stringent test of the theory is provided by comparing the δ values calculated from the slopes of the lines in Figs. 3b and 4b with the theoretical values given by Eq. (16). The theoretical and numerical values of δ obtained in this way are: 0.080 and 0.085 for w = 6.0 m s^{-1}; 0.33 and 0.35 for w = 0.2 m s^{-1}. Corresponding values for intermediate vertical air velocities for which figures are not given are: 0.20 and 0.20 for w = 1.0 m s^{-1}; 0.26 and 0.28 for w = 2.0 m s^{-1}. Thus, there is very good agreement between the theoretical and numerical values of δ.

A more readily appreciated measure of the magnitude of the increase in the width of the distribution due to the surface tension effect is given by the ratio $R = (r_L^2 - r_S^2)/(r_{L0}^2 - r_{S0}^2)$, where r_L and r_S are the radii of the drops grown on the largest nucleus (used in the calculations) and the smallest activated nucleus (that is subsequently not deactivated) at a height z and r_{L0} and r_{S0} are corresponding radii at a lower height z_0. If solute and surface tension effects are neglected then this ratio would be unity for all z, $z_0 > z_m$. With surface tension included the ratio increases with the height z. From the numerical calculations we find for z = 3 km and z_0 = 20 m that R = 1.57, 3.31, 4.48 and 7.42 for w = 6.0, 1.0, 0.5 and 0.2 m s^{-1}, respectively. Thus, the effect of the surface tension in widening the distribution increases with decreasing vertical air velocity as implied by Eqs. (16) and (21).

From the agreement between the results of theory and numerical calculations, we can draw the following conclusions. 1) even after t_m, it is not always a good approximation to neglect the surface tension effect; the neglect has the consequence that the concentration density of drops expressed as a function of r^2 simply translates along the r^2 axis as time increases. When surface tension is included, the width of the distribution increases as it translates along the r^2 axis. This is schematically illustrated in Fig. 1, which shows the concentration density at an initial time (thin solid curve labeled t_0) and at a later time with the surface tension and solute effects neglected (thin solid curve labeled t) and with the surface tension included (thick solid curve labeled t). 2) The increase in the width of the distribution as measured by the increase in var(r^2) is primarily due to the effect of surface tension on the equilibrium vapor pressure over drops.

A potentially important result worth noting in Fig. 4b is that nuclei categories 81 and 83, which are activated near the point of maximum supersaturation, are

later deactivated. Drops growing on nucleus category 82, not plotted in the figure, evidently must suffer a similar fate. Briefly, the reason for this behavior is as follows. At time t_m, or shortly before, nucleus category 83 (for example) is activated. At the time of activation, the equilibrium supersaturation over drops of this nucleus category is equal to or less than s_m. After t_m the ambient supersaturation begins to decrease; the equilibrium supersaturation over drops of this category also begins to decrease as the drops grow beyond their critical radius. However, the ambient supersaturation apparently decreases faster than the equilibrium supersaturation, and at some later time the ambient supersaturation falls below the equilibrium supersaturation. As a result, the drops starts evaporating and are eventually deactivated. In the present example, the nucleus categories 81 and 83 are deactivated at heights of approximately 20 and 600 m, respectively. One consequence of the deactivation is that the value of δ must change at the points of deactivation [see Eq. (16)]. A careful examination of data on which Fig. 4b is based has shown that the slope of the Δ curves do change at those points. The deactivation of previously activated nuclei may have important consequences for the size distribution of cloud drops growing by condensation; it is proposed to discuss it at length in a subsequent communication. The question may be asked: why was this behavior not noted in earlier work? The answer is probably, because enough resolution was not used to describe the nucleus size distribution in those calculations.

4. Discussion

We shall now use the above results to discuss the colloidal stability of warm clouds; a method of including detailed microphysics of the condensation process in cloud dynamics models will also be suggested.

a. Colloidal stability of warm clouds

The colloidal stability of warm clouds is determined mainly by the following characteristics of the drop size distribution: the water content, the average drop size, and the width. In the following we consider distributions of comparable water contents; therefore, we need consider only the average drop size and the width; further, the average drop size and total drop concentration can be used interchangeably. The colloidal instability should increase with average size (that is, decreasing concentration) and width because as the former increases the sweep-out area and the collision efficiency increase and as the later increases the differential fall speeds between the drops increase.

Squires (1958a,b) discussed the colloidal stability of "dark" stratus, Hawaiian orographic cloud, and maritime, transitional and continental cumuli. This series of clouds is known to be generally more stable as one progresses from the stratus to the continental cumulus. From observations of the microstructure of these clouds, Squires (1958a) found that the total drop concentration increased from the stratus to the continental cumulus (the water contents were comparable). He also observed that distributions with lower concentrations tended to be wider. Thus, our expectations of the dependence of colloidal stability on cloud microstructure are confirmed by Squires' observations.

In his second paper, Squires considered the reasons for the differences in the microstructure between the different cloud types. He obtained an approximate analytical solution for the total drop concentration and showed that a smaller vertical air velocity tends to favor a smaller drop concentration. Since the stratus and orographic clouds generally have smaller vertical air velocities, this helps us understand the greater instability of these clouds from the point of view of the effect of drop concentration on stability in terms of a macroscopic cloud characteristic. For a nucleus distribution obeying Eq. (18), these results were further solidified by Twomey (1959) who obtained an approximate analytical solution relating the drop concentration to the vertical air velocity and the nucleus distribution parameters α and β. However, neither of these authors explained the observed association between drop concentration and distribution width nor did they discuss the factors that might control the width. Using the results derived in section 2b, we can now provide partial answers to both of these questions.

In section 2b, we derived an approximate analytical expression for $\mathrm{var}(r^2)$. We first note that for a discussion of the colloidal stability of warm clouds $\mathrm{var}(r^2)$ is the most appropriate measure of the width of the distribution. This is because the terminal fall speed of a cloud drop is proportional to the square of its radius; therefore, $\mathrm{var}(r^2)$ will be proportional to the variance of the fall speeds of the cloud drops and, other things being equal, the latter variance gives a direct measure of the rate of collisions between drops insofar as the width of the distribution is concerned. If we make the approximation of neglecting the effects of surface tension and solute on the equilibrium vapor pressure over drops, then the variance would remain constant with the height [Eq. (9)]. The cloud can then be destabilized only by increases in the cloud water content and the average drop size (East 1957). In actuality, since the surface tension is always operative, $\mathrm{var}(r^2)$ increases with the height. As shown in the previous section, in a stratiform cloud, the variance can increase by a factor of more than 7 over a depth of 3 km; such an increase can obviously have important consequences for the growth of drops by collisions due to differential fall speeds. A measure of the rate of increase of $\mathrm{var}(r^2)$ is given by δ [Eq. (17)], a greater δ implying a faster rate of increase of the variance. Thus, we can say that for

a given cloud water content, a small drop concentration (N) and a large δ both favor colloidal instability, the former through its effect on the average drop size and the latter through its effect on the width of the distribution.

Let us suppose that the nucleus distribution obeys Eq. (18). Then N and δ depend upon three independent variables, namely, w, α and β; therefore, in general, we cannot have a one-to-one relationship between N and δ. To proceed further, we assume that α and β are given. Then the total drop concentration N is proportional to $w^{3\beta/(2\beta+4)}$ [Eq. (19)]. This means that N decreases with decreasing vertical air velocity but slower than w^1 provided $0 < \beta < 4$. Since for observed distributions, this is generally the case (indeed, usually $0 < \beta < 1.2$, see, for example, Braham 1976, Fig. 1), we see from Eq. (16) that decreasing vertical air velocity also implies increasing δ. If we assume a Junge-type nucleus distribution, then $N \propto w^{3/4}$ (see Squires 1958b); thus, in this case also decreasing vertical air velocity implies decreasing N and increasing δ. Therefore, in both cases, clouds with smaller vertical air velocity tend to have smaller drop concentrations and wider distributions. This gives us a partial explanation for Squires' observation that clouds with lower drop concentrations generally have wider distributions. It also shows that clouds with smaller vertical air velocities, such as the dark stratus and the Hawaiian orographic, tend to be more unstable not only because they have lower drop concentrations but also because they tend to have wider drop size distributions.

In the above, we were careful to state that a greater δ provides only a partial explanation for a wider distribution. This is because δ actually gives a measure of the rate of increase of the *ratio* of the variance at any greater height to that at an initial height $> z_m$ [Eq. (17)], and we did not discuss the factors controlling the initial variance. We may also note that using Eqs. (19) and (21) and considering the full dependence of N and δ on w, α and β, it may be possible to give a more complete discussion of the colloidal stability of clouds and, in particular, the reasons for the observed stabilities of the maritime, transitional and continental cumuli. However, this will not be pursued here.

b. *Treatment of the microphysics of condensation in numerical models of cloud dynamics*

For reasons of available computer power, the microphysics of condensation is usually simplified in numerical cloud models, especially multidimensional models. The most extensively used simplification assumes that 1) the vapor in excess of saturation condenses instantly and 2) the development of raindrops from cloud drops may be described by an "autoconversion" parameter (for example, Srivastava 1967). The former assumption gives an excellent approximation for the cloud water content except very near the cloud base. It is much more difficult to improve on the second simplification, because it involves improving the treatment of the evolution of the cloud drop size distribution. In one approach, which is exemplified by the work of Clark (1974, 1976), it is assumed that the cloud drop size distribution may be represented by an analytical expression having a few parameters and equations for the parameters are derived using the condensational growth equations. The equations for the parameters are then solved numerically in the cloud model. This method suffers from the obvious shortcoming that it forces the drop size distribution to conform to a certain predetermined form. More ambitious treatments compute the evolution of the size distribution but, for reasons of available computer power, simplify the growth equations by neglecting the effects of surface tension and solute on the equilibrium vapor pressure over drops (for example, Hall 1980; Song and Marwitz 1989). As we have discussed, neglect of the solute effect after t_m may be defensible but neglect of the surface tension effect produces drop size spectra that err on the side of being too narrow, especially in weak updrafts. (In practice, however, spreading of the size distribution by the finite difference methods used for the numerical calculations may produce quite the opposite effect.) We suggest that using the equations derived in section 2b and their extension to variable updrafts discussed below, we can retain the surface tension effect and thereby treat the condensation process more accurately in numerical cloud models. The proposed method can be used only after t_m. Before t_m and at the time when nuclei may be activated or deactivated, the size distribution would need to be calculated by other methods, perhaps solution of the full equations of condensational growth.

Consider first the case of a constant updraft. Let the size distribution at an initial time t_0 and a later time t be denoted by $n(r_0^2)$ and $n(r^2)$, respectively. These two distributions are related by

$$n(r^2) = n(r_0^2)\frac{dr_0^2}{dr^2} \tag{22}$$

and the radii at the two times are related by [see Eq. (15)]:

$$(r^2 - r_1^2) = \left(\frac{t}{t_0}\right)^{\delta}(r_0^2 - r_{10}^2). \tag{23}$$

Here r, r_0 and r_1, r_{10} are corresponding pairs of radii at times t and t_0, respectively. The derivative in (22) can be found from (23). We can calculate the size of any drop at the later time, that is, given r_0 we can calculate r, provided we know that relationship for any other size category (specified here by the subscript 1); this relationship is determined by the requirement that

the water content under the distribution $n(r^2)$ equal the water content given by the equations for balance of water substance used in the cloud model. Thus, (22) and (23), together with equations for the balance of water substance, can be used to calculate $n(r^2)$ from $n(r_0^2)$. Because this method is analytical and does not require finite differencing, it has the advantages that 1) it may not be computationally as intensive as finite difference methods and 2) it may not suffer from numerical spreading common to most finite difference methods.

We now consider the case of a nonuniform vertical air velocity. We approximate the vertical air velocity by piecewise constant or piecewise linear functions over small increments of the height (for example, the vertical grid interval in the case of a numerical cloud model). Equation (22) still holds with the subscript 0 signifying the initial level and unsubscripted variables referring to the next height level. In this case, Eq. (14) is replaced by

$$l = l_0 + \frac{a_1}{a_2} z \tag{24}$$

and Eq. (13) is replaced by

$$\frac{d \ln \Delta}{dt} = w \frac{4\pi\rho_w}{3} \frac{NcP}{l_0 + (a_1/a_2)z}. \tag{25}$$

This equation can be integrated to give

$$\frac{r^2 - r_1^2}{r_0^2 - r_{10}^2} = \frac{4\pi\rho_w}{3} NcP \int \frac{wdz}{l_0 + (a_1/a_2)z} \tag{26}$$

where the integral is taken over the height interval under consideration. For a constant or linearly varying vertical air velocity the integral on the right-hand side can be evaluated in closed form. This gives us a generalization of Eq. (23) to variable vertical air velocity; the procedure described above for the case of a constant vertical air velocity can now be carried through for the more general case also. This completes our suggested treatment of cloud microphysics in numerical cloud models.

5. Summary

We have discussed the growth of cloud drops by condensation in a closed air parcel. Two important characteristics of the cloud drop size distribution are the total drop concentration and the width of the distribution. Past work yielded an approximate analytical solution relating the drop concentration to the vertical air velocity and the coefficient α and exponent β of the power-law supersaturation spectrum (18) (Twomey 1959). Past work on the width of the distribution made the approximation of neglecting the effects of surface tension and solute on the equilibrium vapor pressure over drops after the point of maximum supersaturation. Using this approximation, it was shown in the past work that the difference of squared radii of any two given cloud drops and the variance of square radius of the drop size distribution remain constant after the point of maximum supersaturation. Here, we have obtained an improved approximate analytical solution for the width of the distribution by including the surface tension effect even after the point of maximum supersaturation. According to this solution, the difference of squared radii of any two given cloud drops and the variance of square radius of the drop size distribution increase with the progress of condensation. The increases have been related to the vertical air velocity and the parameters α and β of the nucleus spectrum (18). The increases are more pronounced in clouds having low vertical air velocities and high drop concentrations. The improved analytical solution for the width of the distribution has been verified by calculations in which both surface tension and solute effects were included. Since the analytical solution considered only the surface tension effect, this verification also implies that the increase in the variance is primarily due to the surface tension effect.

The approximate solution for the width of the distribution has been used to discuss the colloidal stability of warm clouds from the point of view of the width of the distribution. A partial explanation has been given for the observation that cloud drop size distributions having small drop concentrations tend to be wider. A procedure for a more accurate treatment of the microphysics of condensation in numerical cloud models has been suggested.

The numerical calculations have shown that the generally accepted result that at the point of the maximum supersaturation the condensation nuclei divide into two groups one of which continues to grow and the other slowly decreases in size may need to be modified. This is because drops growing on some of the nuclei that are activated at or near the point of maximum supersaturation may subsequently become deactivated as the ambient supersaturation starts to decrease; this effect may also be especially important in clouds having weak vertical air velocities.

Acknowledgments. This research was supported by the National Science Foundation under Grant ATM 89 03683. Mr. John Valdes provided invaluable assistance with the calculations and the figures.

REFERENCES

Braham, R. R., 1976: CCN spectra in C–k space. *J. Atmos. Sci.*, **33**, 343–345.

Clark, T. L., 1974: A study in cloud phase parameterization using the gamma distribution. *J. Atmos. Sci.*, **31,** 142–155.

——, 1976: Use of log-normal distributions for numerical calculations of condensation and coalescence. *J. Atmos. Sci.*, **33,** 810–821.

East, T. W. R., 1957: An inherent precipitation mechanism in cumulus clouds. *Quart. J. Roy. Meteor. Soc.*, **83,** 61–76.

Hall, W. D., 1980: A detailed microphysical model with a two-dimensional dynamic framework: Model description and preliminary results. *J. Atmos. Sci.*, **37,** 2486–2507.

Howell, W. E., 1949: The growth of cloud drops in uniformly cooled air. *J. Meteor.*, **6,** 134–149.

Johnson, D., 1980: The influence of cloud-base temperature and pressure on droplet concentration. *J. Atmos. Sci.*, **37,** 2079–2085.

Kovetz, A., 1969: An analytical solution for the change in cloud and fog droplet spectra due to condensation. *J. Atmos. Sci.*, **26,** 302–304.

Mason, B. J., 1971: *The Physics of Clouds.* Clarendon Press, 671 pp.

Pruppacher, H. R., and J. D. Klett, 1978: *Microphysics of Clouds and Precipitation.* D. Reidel, 714 pp.

Rogers, R. R., and M. K. Yau, 1989: *A Short Course in Cloud Physics.* Pergamon Press, 209 pp.

Song, N., and J. Marwitz, 1989: A numerical study of the warm rain process in orographic clouds. *J. Atmos. Sci.*, **46,** 3479–3486.

Squires, P., 1958a: The microstructure and colloidal stability of warm clouds. Part I—The relation between structure and stability. *Tellus,* **10,** 256–261.

——, 1958b: The microstructure and colloidal stability of warm clouds. Part II—The causes of variations in microstructure. *Tellus,* **10,** 262–271.

Srivastava, R. C., 1967: A study of the effect of precipitation on cumulus dynamics. *J. Atmos. Sci.*, **24,** 36–45.

——, 1989: Growth of cloud drops by condensation: A criticism of currently accepted theory and a new approach. *J. Atmos. Sci.*, **46,** 869–887.

Twomey, S., 1959: The nuclei of natural cloud formation. Part II: The supersaturation in natural clouds and the variation of cloud droplet concentration. *Geofis. Pura. Appl.*, **43,** 243–249.